Keller et al., http://www.jcb.org/cgi/content/full/jcb.201307049/DC1

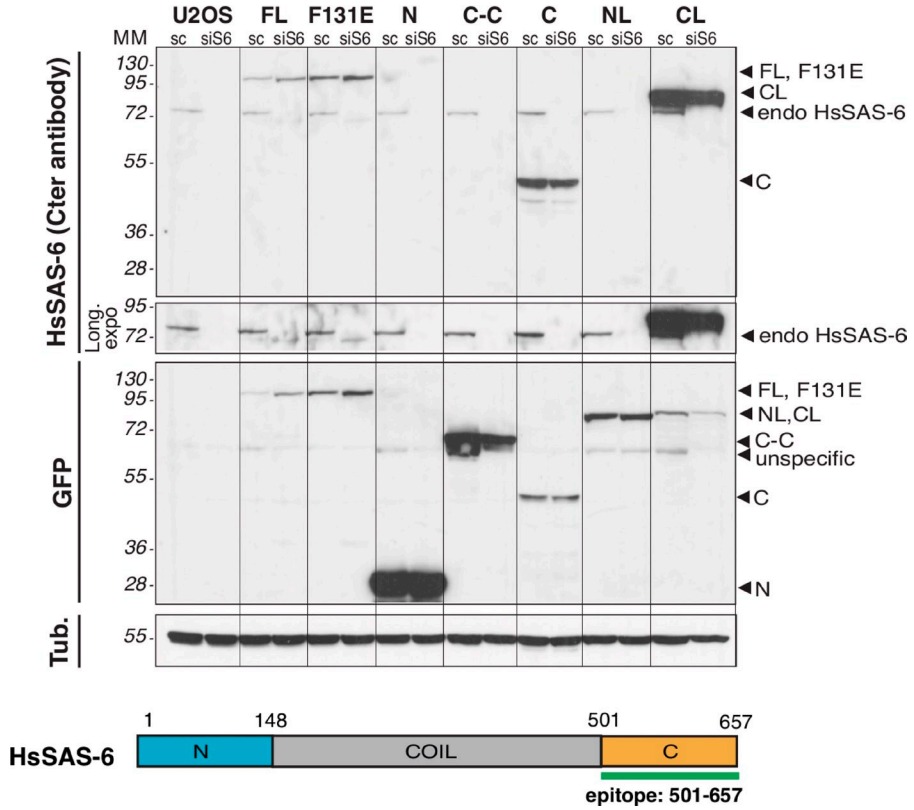

Figure S1. **Exogenous HsSAS-6 variants characterization and antibody specificity.** (A) Western blot analysis of protein extracts from iU2OS cells expressing the indicated constructs and treated with control siRNA (sc) or siHsSAS-6 3′UTR (siS6), using mouse HsSAS-6 (top), rabbit GFP (middle, to control for expression of all the constructs), and α-tubulin antibodies (bottom). Differences in expression levels between constructs are inherent to the episomal expression system (Bach et al., 2007). Treatment with siHsSAS-6 3′UTR leads to efficient depletion of endogenous HsSAS-6 (see longer exposure [Long. expo]) but not of the different variants, lacking the 3′UTR and thus resistant to this siRNA. Note that the monoclonal HsSAS-6 antibody, which was raised against amino acids 404–657 (Kleylein-Sohn et al., 2007), recognizes only endogenous HsSAS-6, FL-GFP, F131E-GFP, GFP-C, and GFP-CL. Given the signal intensity of GFP-CL versus GFP-C, we cannot exclude that part of the epitope lies at the boundary between the coil and the C-terminal fragments. However, because of the lack of HsSAS-6 signal with GFP–C-C, the epitope recognized by this monoclonal antibody most likely lies solely in the C-terminal moiety of HsSAS-6, between residues 501 and 657 (see schematics below). Predicted molecular masses are ∼103 kD for FL-GFP, ∼45 kD for GFP-N, ∼70 kD for GFP–C-C, ∼48 kD for GFP-C, and ∼74 kD for HsSAS-6. Schematics of HsSAS-6 domain organization (N, C-C, and C), showing fragments used for Western blot analysis. The C-terminal epitope recognized by the antibody used in this study (including 3D-STORM experiments) is indicated by the green line. Black lines indicate that intervening lanes have been spliced out. Cter, C terminus; Tub, tubulin; MM, molecular mass; endo, endogenous.

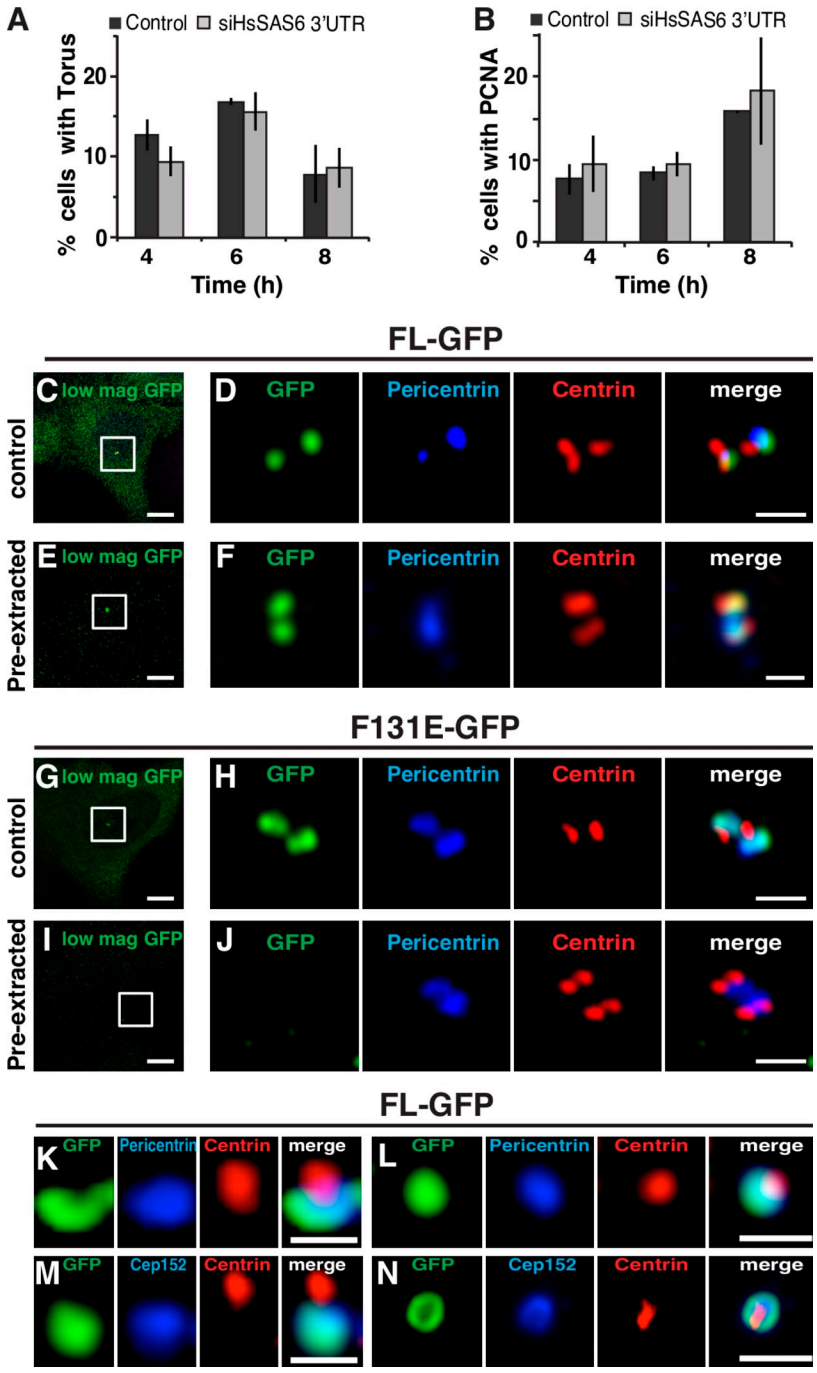

Figure S2. **FL-GFP and F131E-GFP localize at the proximal end of the parental centriole within a detergent-sensitive torus.** (A and B) iU2OS cells expressing FL-GFP were induced with doxycycline for 48 h concomitant to control siRNA (Lo GC) or siHsSAS-6 3′UTR treatment, synchronized by mitotic shake off, fixed at the indicated times, and stained for GFP, centrin, and PCNA as an S-phase marker. The occurrence of the FL-GFP torus and percentage of PCNA-positive cells in control and siRNA-treated cells was calculated at the indicated times. Error bars show standard error of the mean; number of cells analyzed from at least two experiments are reported in Table S2. (C–J) Stability of the torus at centrioles was analyzed in untreated or preextracted cells expressing FL-GFP (C–F) or F131E-GFP (G–J), which were fixed and labeled with GFP, centrin, and Pericentrin. Low magnification images (low mag.) illustrate decrease in cytosolic GFP signal after treatment. Comparison of the GFP signal reveals that the F131E-GFP signal is completely lost from centrioles but not FL-GFP, which is presumably stably incorporated. Insets are magnified regions of the boxed areas. (K–P) Cells expressing FL-GFP were synchronized by mitotic shake off, fixed 6 h thereafter, and labeled with GFP, Pericentrin, and centrin-2 (K and L) or Cep152 and centrin-2 (M and N). Bars: (C, E, G, and I) 10 µm; (D, F, H, and J) 1 µm; (K–N) 500 nm.

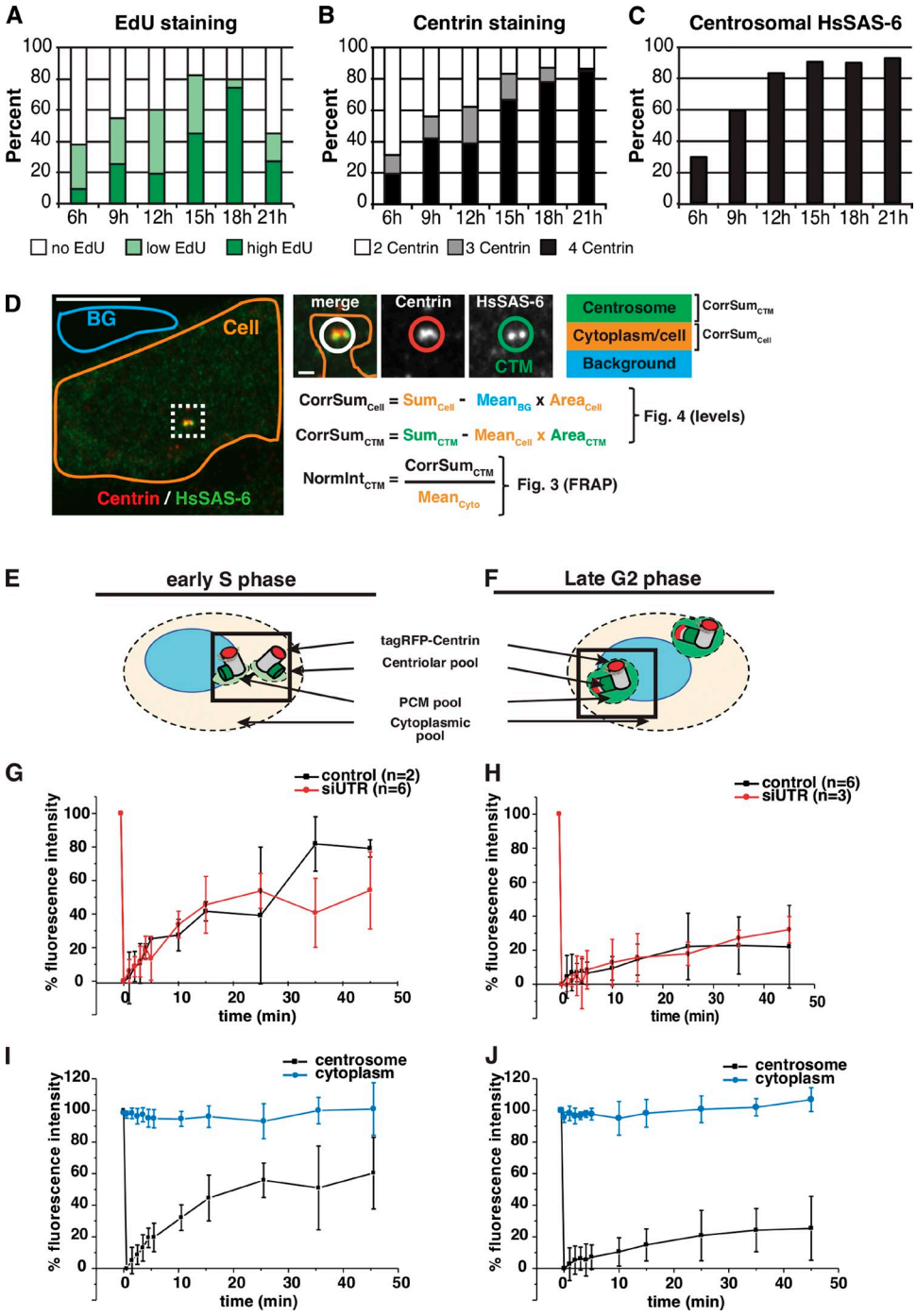

Figure S3. **Synchronization protocol and fluorescence intensity quantification procedure.** (A–C) U2OS cells were synchronized by mitotic shake off and analyzed at successive time points thereafter, monitoring entry into S phase by EdU incorporation (A), the number of centrin foci (B), or the presence of centrosomal HsSAS-6 to monitor centriole duplication (C). Note that the data of A and B come from the same cells, and that from C come from other ones. Number of cells for A and B: n = 107 for 6 h, n = 155 for 9 h, n = 206 for 12 h, n = 106 for 15 h, n = 78 for 18 h, n = 67 for 21 h, and n = 83 for 24 h; for C: n = 81 for 6 h, n = 66 for 9 h, n = 71 for 12 h, n = 94 for 15 h, n = 87 for 18 h, and n = 82 for 21 h. (D) Illustration of the regions used for the quantification of HsSAS-6 total cellular and centrosomal intensity: background (BG; outside the cell), cell (covering the entire cytoplasm), and centrosome. For the centrosomal region, a circle (22 px for FL-GFP recovery after FRAP in Fig. 3 C or 20 px for HsSAS-6 levels analysis in Fig. 4 E) was placed above the centrosome using the centrin signal to center the region. For all three regions, the mean, sum of intensities, and areas were measured in Fiji and used to calculate the corrected intensities as described by the indicated formulas (Materials and methods). Note that the cellular area (unbleached background) in the FRAP analysis did not contain the bleached centrosomal region (dotted square), and the centrosomal intensity was further normalized to the mean cytoplasmic intensity to account for photobleaching during the acquisition. Bars: (main image) 10 µm; (insets) 1 µm. (E and F) Schematics of early S and late G2 cells illustrating the number of centrioles (tagRFP-centrin, red) and the different HsSAS-6 pools (centriolar, dark green; PCM, light green; cytoplasmic, yellow). Nucleus is blue. (G and H) Fluorescence intensity recovery after photobleaching in control cells and siHsSAS-6–treated cells (siUTR) in early S phase (G) or late G2 (H) indicates no or little difference between the two datasets that were subsequently pooled. Number of cells is indicated on the graph. (I and J) Fluorescence intensity curves from pooled cells (control and siRNA treated), comparing centrosomal intensity after photobleaching (black) to cytoplasmic intensity in unbleached region (blue) in early S (n = 8; I) and late G2 (n = 9; J) and illustrating little or no photobleaching. Protein production that would have occurred within the 45-min-long experiments was not considered. Curves represent mean normalized intensity; error bars show standard deviations.

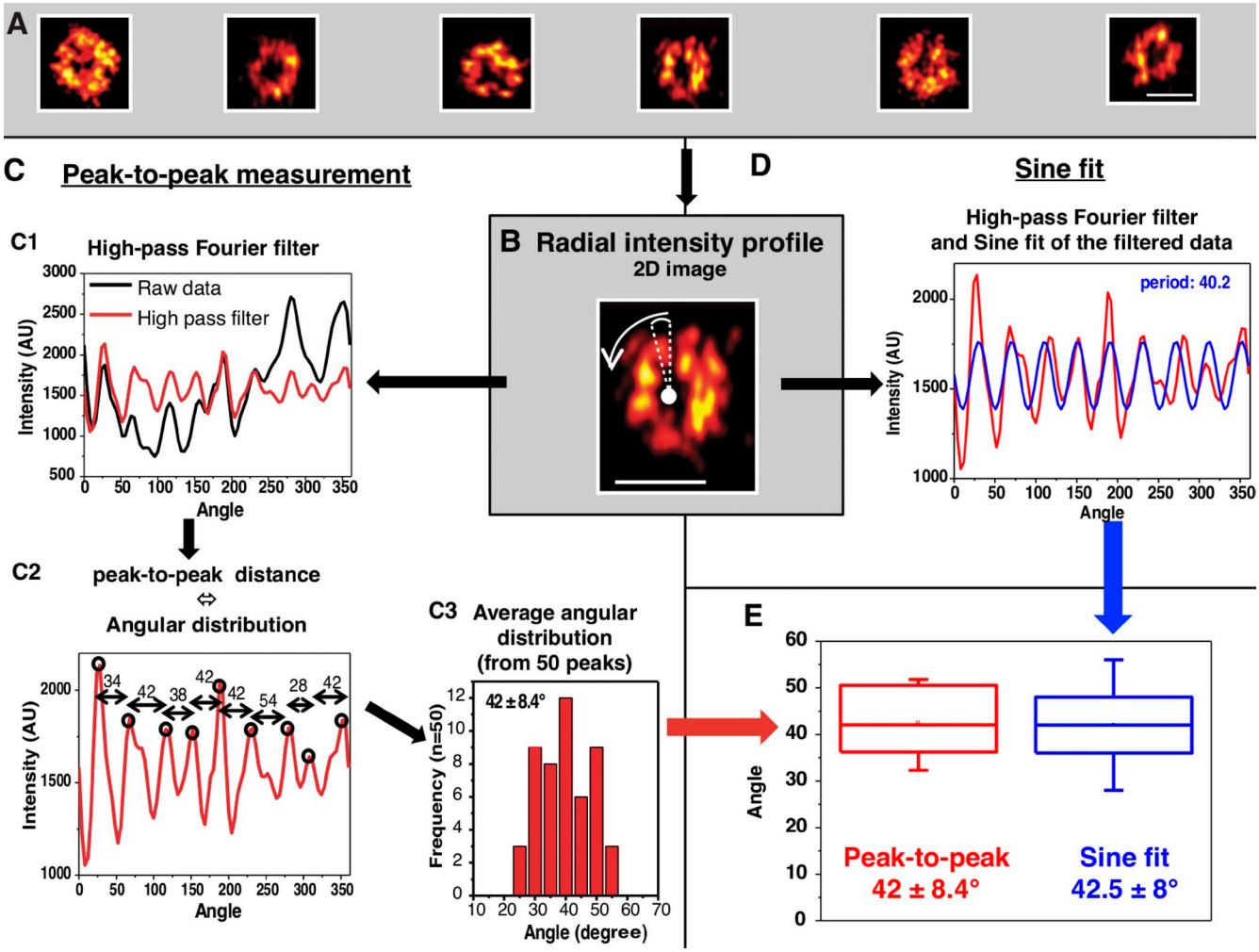

Figure S4. **Determination of angular distribution of HsSAS-6 rings.** (A) 2D projection of each centriole analyzed in these 3D-STORM experiments; data of a single centriole (boxed) is taken for illustration purposes of the two methods that were used. (B–D) Illustration of the radial intensity sampling along the circumference of the ring (B) and the estimation of the angular distribution from radial peak-to-peak measurements (C) or using sine fitting (D). (C) The radial intensity curve (black) was treated using a high-pass Fourier filter to remove low-frequency modulations (red curve) followed by determination of the distance between two peaks corresponding to an angular value (C2); the resulting angular distribution of the 50 peaks derived from the centrioles shown in A is then plotted (C3), and calculated mean angle ± standard deviation is indicated. (D) The procedure is similar as in C, but here, the filtered data are fitted by a single sine function (blue curve), yielding a mean angular period value. (E) Both measurements yield similar angular distributions from all six centrioles analyzed, which are consistent with a ninefold symmetry (corresponding to a 40° angle) as shown in the box plot (as in Fig. 6). Box plots represent lower and upper quartiles and median values (horizontal line) as well as the standard deviations. AU, arbitrary unit. Bars, 100 nm. Note that the representation of the imaged centrioles in A can appear tilted as a result of the projection in 2D of a 3D structure.

Table S1. **Cell numbers (Fig. 1)**

Categories	U2OS	FL	N	C-C	C	NL	CL
S phase	Strnad et al., 2007	24	ND	20	ND	20	20
Mitosis	Strnad et al., 2007	41	ND	40	ND	86	48
Control	337	–	–	–	–	–	–
siUTR	452	313	140	89	95	114	100

Numbers of S phase and mitotic cells analyzed for centrosomal GFP signal in Fig. 1 are indicated when appropriate. Function of individual HsSAS-6 variants was assessed comparing cells in mitosis depleted of HsSAS-6 (siUTR) or untreated (control).

Table S2. **Cell numbers after shake off and results of two-way ANOVA (Fig. S2)**

Time/*n*	Torus			PCNA		
	Control	siUTR	P-value	Control	siUTR	P-value
h						
4	287	227	0.7403	366	339	0.9707
6	264	255	0.9826	270	272	0.9929
8	262	332	0.9905	241	277	0.929
Two-way ANOVA	0.6544			0.6813		

Number of analyzed cells (*n*) at successive times after shake off (hours) after Lo GC negative control siRNA (control) and siHsSAS-6 3′UTR (siUTR) treatment scoring for prevalence of torus (Torus) or percentage of PCNA-positive cells (PCNA). Results of two-way ANOVA test ($\alpha = 0.05$; p-value is indicated below each column) show no significant differences, as show the corrected p-values from multiple comparisons between conditions and at a given time point.

Table S3. **Results of Kruskal–Wallis test ($\alpha = 0.05$; Fig. 4 E)**

Stage of comparison	Early S	S–G2	Late G2	*n*
G1	> 0.9999 ns	0.0515 ns	<0.0001****	8
Early S		0.3173 ns	0.0014**	5
S–G2			0.0428*	27
Late G2				14

P-values from Kruskal–Wallis multiple comparisons ($\alpha = 0.05$) on total HsSAS-6 cellular intensity from Fig. 4 E, showing increasing significance (number of asterisks). Number of cells analyzed (*n*) are indicated in right-most column.

Table S4. **Results of ANOVA ($\alpha = 0.05$; Fig. 4 F)**

Stage of comparison	Early S	S–G2	Late G2	n_{CTM}/n
G1	0.2038 ns	<0.0001****	<0.0001****	13/8
Early S		0.05 ns	<0.0001****	8/7
S–G2			<0.0001****	53/27
Late G2				28/14

P-values from ANOVA multiple comparisons ($\alpha = 0.05$) on centrosomal HsSAS-6 intensity from Fig. 4 F, showing increasing significance (number of asterisks). Number of cells analyzed (*n*) or number of centrosomes (n_{CTM}) are indicated in right-most column.

Table S5. **Results of Kruskal–Wallis test (α = 0.05; Fig. 5 E)**

Stage of comparison	GFP–GFP	FL	F131E	C	*n*
GFP	<0.0001****	<0.0001****	<0.0001****	>0.9999 ns	29
GFP–GFP		0.0069**	0.0184*	<0.0001****	40
FL			>0.9999 ns	0.0006**	43
F131E				<0.0001****	49
C					27

P-values from Kruskal–Wallis multiple comparisons (α = 0.05) on normalized brightness from Fig. 5 E, showing increasing significance (number of asterisks). Number of cells analyzed (*n*) are indicated in right-most column; the same cells were used for Fig. 5 (C and D) and Table S5 and Table S6.

Table S6. **Results of Kruskal–Wallis test (α = 0.05; Fig. 5 F)**

Stage of comparison	GFP–GFP	FL	F131E	C	*n*
GFP	0.0220*	<0.0001****	<0.0001****	>0.9999 ns	29
GFP–GFP		<0.0001****	<0.0001****	>0.9999 ns	40
FL			>0.9999 ns	<0.0001****	43
F131E				<0.0001****	49
C					27

P-values from Kruskal–Wallis multiple comparisons (α = 0.05) on diffusion coefficient values from Fig. 5 F, showing increasing significance (number of asterisks). Number of cells analyzed (*n*) are indicated in right-most column; the same cells were used for Fig. 5 (C and D) and Table S5 and Table S6.

Table S7. **Primer name and sequence to generate specific entry vectors**

Vector name	Forward primer (5′ → 3′)	Reverse primer (5′ → 3′)	Boundaries
			AA
pENTR-FL	CGCGACCGGTACCATGAGCCAAGTGCTGTTCCAC	CGCGTCTAGATAACTGTTTGGTAACTGCCCA	1–657
pENTR-N	CGCGACCGGTACCATGAGCCAAGTGCTGTTCCAC	CGCGTCTAGATATTAATCATCTAGTGATTGCATC	1–173
pENTR-C-C	CGCGACCGGTACCATGGAGATAAAGAAATTTCTC	CGCGTCTAGATATTAGCTGCTGGAATGTGCAGG	148–501
pENTR-C	CGCGACCGGTACCATGGAACTAAATGAAAATCAG	CGCGTCTAGATTAACTGTTTGGTAACTGCCCA	477–657
pENTR-NL	CGCGACCGGTACCATGAGCCAAGTGCTGTTCCAC	CGCGTCTAGATATTAGCTGCTGGAATGTGCAGG	1–501
pENTR-CL	CGCGACCGGTACCATGGAGATAAAGAAATTTCTC	CGCGTCTAGATTAACTGTTTGGTAACTGCCCA	148–657

Name of primers used for generating entry vectors for the different constructs, along with primer sequences (5′ to 3′); restriction sites are underlined. The stop codon for N-terminal fusions was added to the primer. Amino acid boundaries (AA) are indicated for each variant.

References

Bach, M., S. Grigat, B. Pawlik, C. Fork, O. Utermöhlen, S. Pal, D. Banczyk, A. Lazar, E. Schömig, and D. Gründemann. 2007. Fast set-up of doxycycline-inducible protein expression in human cell lines with a single plasmid based on Epstein-Barr virus replication and the simple tetracycline repressor. *FEBS J.* 274:783–790. http://dx.doi.org/10.1111/j.1742-4658.2006.05623.x

Kleylein-Sohn, J., J. Westendorf, M. Le Clech, R. Habedanck, Y.-D. Stierhof, and E.A. Nigg. 2007. Plk4-induced centriole biogenesis in human cells. *Dev. Cell*. 13:190–202. http://dx.doi.org/10.1016/j.devcel.2007.07.002

Strnad, P., S. Leidel, T. Vinogradova, U. Euteneuer, A. Khodjakov, and P. Gönczy. 2007. Regulated HsSAS-6 levels ensure formation of a single procentriole per centriole during the centrosome duplication cycle. *Dev. Cell*. 13:203–213. http://dx.doi.org/10.1016/j.devcel.2007.07.004